Proceedings of the 2005 IEEE
International Conference on Robotics and Automation
Barcelona, Spain, April 2005

Stable Haptic Display of Slowly Updated Virtual Environment with Multirate Wave Transform

Changhyun Cho, and Munsang Kim
Center for Intelligent Robotics
39-1, Hawolgok-dong, Seongbuk-gu, Seoul, 136-791, Korea
{chcho, munsang}@kist.re.kr

Chang-Soon Hwang, and Jaehyung Lee
Intelligent Robotics Research Center
Korea Institute of Science and Technology
39-1, Hawolgok-dong, Seongbuk-gu, Seoul, 136-791, Korea
{cshwang, quarky}@kist.re.kr

Jae-Bok Song
Dept. of Mechanical Eng
Korea University
5, Anam-dong, Seongbuk-gu, Seoul, 136-701, Korea
jbsong@korea.ac.kr

***Abstract* - This paper proposes a control method that overcomes the instability arising from both the low update rates of the virtual environment (VE) and the time delay in a communication line. The instability arising from the time delay in a communication line can be overcome using the wave variables since time delay on the wave variables is passive. The so-called multirate control scheme is applied to cope with the problems presented by the low update rates of VE. Since digital sample and hold (rate transitions) can be represented as a series of time delay, the passive nature of time delay on the wave variables is applied. By computing the norm of the scattering matrix, it was verified that rate transitions on the wave variables are passive, thereby deriving a stable haptic interface with the multirate wave transform. Various experiments have shown that a stable force display is achieved with the multirate wave transform.**

Index Terms* - *Multirate wave transform, wave variables, scattered network, low update rate.

I. INTRODUCTION

In some cases, haptic interfaces become unstable due to the presence of active elements, such as time delay in communication line and sampling [1]. Oscillatory motion is often observed with active elements.

Many studies have been conducted in order to cope with this unstable behavior caused by active elements. The so-called virtual coupling has been implemented between the haptic device and the virtual environment (VE) [2-4]. Damping elements are usually applied to the virtual coupling to stabilize a haptic interface. Colgate and Schenkel [2] derived a parameter range of virtual coupling using the dynamic model of a haptic device that guarantees the stability of sampled-data systems. Adams and Hannaford [3] suggested a design scheme of virtual coupling, which can derive optimal parameters of virtual coupling using the dynamic model of a haptic device. Miller et al. [4] also developed a design method for nonlinear environments, in which several conditions for parameters of virtual coupling were presented.

The above algorithms required a precise model or a measured damping coefficient of a haptic device in order to determine the proper parameters for virtual coupling. Several research studies have also been carried out without resort to any information of a haptic device. Hannaford and Ryu [5] suggested an energy-based scheme in which a passivity observer measured energy in real time and a passivity controller adjusted a controllable dissipation element. Stramigioli et al. [6] presented a discretization technique of port-Hamiltonian systems. In addition, a control method was developed that limits the maximum deviation of energy during the sampling interval, thereby achieving stable haptic display. These algorithms, however, require the determination of an appropriate threshold, which is used to classify energy behavior as stable or unstable behavior and to activate a control action.

In their study, Anderson and Spong [7] revealed that time delay in a scattered network line was passive. Niemeyer and Slotine also worked further on this subject [8, 9] by investigating the application and behavior of wave variables. Secchi et al. [10] presented a discretization technique of a scattered network and showed that a packet loss in the scattered communication line was passive, just like time delay. Although the instability arising from time delay can be overcome, significant position errors between the master- and slave-device usually occur. Hence, much research is being conducted to overcome these position errors [9, 11, 12].

Although the algorithms based on the scattering parameters have shown satisfactory performance, their approaches have been focused on the limitation caused by time delay. A number of physical models in VE are often slowly updated due to the graphic update rate and the computation time of physical laws (e.g., a spring or a damper). It is obvious that the haptic performance (e.g., *Z*-width [13]) is degraded by the slow updating of VE and by time delay in a communication line. It is therefore useful to have a haptic controller that enables fast updating in order to obtain a better inter-sample behavior of a slowly updated VE. To this end, the so-called multirate control scheme widely used in various fields can be employed [14-16].

This paper deals with the instability of a network-based haptic interface due to the low VE update rate and time delay in a communication line. The instability due to the low VE update rate can be resolved by the so-called multirate control scheme, while the time delay in a communication line can be handled by employing the wave variables, since it becomes passive in the scattered network [7-10]. In the conventional multirate haptic system, a damping element is usually implemented as a haptic controller to stabilize the haptic system and rate transitions such as downsampling and upsampling are conducted using the power variables such as velocity and force. This research shows that the rate transitions are active on the power variables, while passive on the wave variables as is the case with the time delay.

By conducting the rate transitions on the wave variables, the so-called multirate wave transform can be formulated. Since this transform naturally generates the

damping effect, stable force display can be achieved without any additional damping elements necessary to stabilize the conventional haptic system. That is, with the multirate wave transform, any extrinsic controller (e.g., added damping) is not necessary to stabilize the haptic systems which tend to become unstable due to the low VE update rate and/or time delay in a communication line. It is shown from experiment that stable force display can be achieved with the multirate wave transform.

II. Conventional Multirate Haptic Interface

To improve the inter-sample behavior of the slowly updated VE, multiple control rates are sometimes applied to a haptic system. This type of system is called a *multirate* system. Suppose that the sampling period, T, of a haptic controller, $G_c(z)$, is less than the update period, T_{ve}, of VE, $G(z_{ve})$, where $z = e^{Ts}$ and $z_{ve} = e^{T_{ve}s}$. Figure 1 depicts this network representation. As shown in the figure, f_h and f_{ve} represent the hand-force input by a human operator and the desired force computed by VE, respectively. $H(s)$ denotes the transfer function of a haptic device, while k and k_{ve} represent the corresponding time index. Let $\dot{x}$ and $\dot{x}_{ve}$ be the velocities of the haptic device and VE, respectively. In Fig. 1, two rate transitions occur: downsampling and upsampling. That is, the haptic controller output $\dot{x}(kT)$ is downsampled to $\dot{x}_{ve}(k_{ve}T_{ve})$, while $f_{ve}(k_{ve}T_{ve})$ is upsampled to $f(kT)$. This paper considers a 1 DOF problem for simple analysis.

Let us investigate the effects of the rate transitions. A multirate form of $\dot{x}(kT)$ can be represented by

$$\dot{x}(kT) = \dot{x}(k_{ve}T_{ve} + iT), \tag{1}$$

where $i = 0, \ldots, n\text{-}1$ and $n = T_{ve}/T$ is an integer. A simplified notation, $\dot{x}(k_{ve}, i)$, will be used for $\dot{x}(k_{ve}T_{ve} + iT)$. The *lifting* technique [17, 18] can be used to represent a finite-dimensional sampled-data system as a time-invariant infinite-dimensional discrete system. Using the lifting operator, $L_{T\to T_{ve}} : l_T^p \to l_{T_{ve}}^p$, $1 \le p \le \bullet$, $\dot{x}(k_{ve}, i)$ can be represented only at the sampling period T_{ve}. For simplicity, let $L_{T_{ve}}$ be $L_{T\to T_{ve}}$. The lifted form of $\dot{x}(k_{ve}, i)$ is defined by

$$\tilde{\dot{x}}(k_{ve},0) = L_{T_{ve}}\dot{x}(k_{ve},i),\ \dot{x}(k_{ve},i) = L_{T_{ve}}^{-1}\tilde{\dot{x}}(k_{ve},0), \tag{2}$$

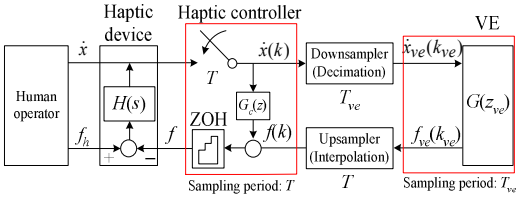

Fig. 1. Multirate haptic interface with a fast haptic controller and slow VE.

where $i = 0, \ldots, n\text{-}1$ and $n = T_{ve}/T$ is an integer. A simplified notation, $\dot{x}(k_{ve}, i)$, will be used for $\dot{x}(k_{ve}T_{ve} + iT)$. The *lifting* technique [17, 18] can be used to represent a finite-dimensional sampled-data system as a time-invariant infinite-dimensional discrete system. Using the lifting operator, $L_{T\to T_{ve}} : l_T^p \to l_{T_{ve}}^p$, $1 \le p \le \infty$, $\dot{x}(k_{ve}, i)$ can be represented only at the sampling period T_{ve}. For simplicity, let $L_{T_{ve}}$ be $L_{T\to T_{ve}}$. The lifted form of $\dot{x}(k_{ve}, i)$ is defined by

$$\begin{aligned}\tilde{\dot{x}}_{ve}(k_{ve},0) &\in R^n \\ &= [\dot{x}_{ve}(k_{ve},0) \quad \dot{x}_{ve}(k_{ve},1) \quad \cdots \quad \dot{x}_{ve}(k_{ve},n-1)]^T \\ &= [\dot{x}_{ve}(k_{ve},0) \quad \dot{x}_{ve}(k_{ve},0) \quad \cdots \quad \dot{x}_{ve}(k_{ve},0)]^T \\ &= [\dot{x}(k_{ve},0) \quad \dot{x}(k_{ve},0) \quad \cdots \quad \dot{x}(k_{ve},0)]^T\end{aligned} \tag{3}$$

Equation (3) can be rewritten with $\tilde{\dot{x}}(k_{ve},0)$ and the series of time delay as follows:

$$\begin{aligned}\tilde{\dot{x}}_{ve}(k_{ve},0) &= [\dot{x}(k_{ve},0) \quad \dot{x}(k_{ve},0) \quad \cdots \quad \dot{x}(k_{ve},0)]^T \\ &= [\dot{x}(k_{ve},0) \quad z^{-1}\dot{x}(k_{ve},1) \quad \cdots \quad z^{-(n-1)}\dot{x}(k_{ve},n-1)]^T\end{aligned} \tag{4a}$$

$$\tilde{\dot{x}}_{ve}(k_{ve},0) = \mathbf{P}\tilde{\dot{x}}(k_{ve},0), \tag{4b}$$

where $\mathbf{P} = \begin{bmatrix} 1 & 0 & \cdots & 0 \\ 0 & z^{-1} & & \vdots \\ \vdots & & \ddots & 0 \\ 0 & \cdots & 0 & z^{-n+1} \end{bmatrix} = \begin{bmatrix} 1 & 0 & \cdots & 0 \\ 0 & z_{ve}^{-\frac{1}{n}} & & \vdots \\ \vdots & & \ddots & 0 \\ 0 & \cdots & 0 & z_{ve}^{-\frac{n-1}{n}} \end{bmatrix} \in R^{n\times n}$ and

$z_{ve} = e^{T_{ve}s} = e^{nTs} = z^n$.

Since $f(k_{ve}, i)$ is obtained from the interpolation (or upsampling) of $f_{ve}(k_{ve}, 0)$, which has a constant value during the sampling period of T_{ve}, then $\tilde{f}(k_{ve},0) = \tilde{f}_{ve}(k_{ve},0)$. Let the input vector be $\mathbf{x} = [\tilde{\dot{x}}(k_{ve},0) \quad \tilde{f}_{ve}(k_{ve},0)]^T \in R^{2n}$ and the output vector be $\mathbf{y} = [\tilde{f}(k_{ve},0) \quad -\tilde{\dot{x}}_{ve}(k_{ve},0)]^T \in R^{2n}$, so that $\mathbf{x}^T\mathbf{y} = \tilde{\dot{x}}(k_{ve},0)^T\tilde{f}(k_{ve},0) - \tilde{\dot{x}}_{ve}(k_{ve},0)^T\tilde{f}_{ve}(k_{ve},0)$ represents the power input of the rate transition. From (4b) and $\tilde{f}(k_{ve},0) = \tilde{f}_{ve}(k_{ve},0)$, the input-output vector can be obtained as follows:

$$\mathbf{H}(z_{ve})\mathbf{x} = \begin{bmatrix} \mathbf{0} & \mathbf{I}_n \\ -\mathbf{P}(z_{ve}) & \mathbf{0} \end{bmatrix}\mathbf{x} = \mathbf{y}, \tag{5}$$

where $\mathbf{I}_n$ is the $n\times n$ identity matrix.

To verify the passivity of the rate transition, the scattering operator is applied [19]. If the operator H maps the input vector to the output vector, the scattering operator is defined by

$$\mathbf{S}(z_{ve}) = [\mathbf{H}(z_{ve}) - \mathbf{I}_{2n}][(\mathbf{I}_{2n} + \mathbf{H}(z_{ve})]^{-1}, \tag{6}$$

where $[\mathbf{I}_{2n}+\mathbf{H}(z_{ve})]$ is invertible. With this definition, the system is passive if and only if $\|\mathbf{S}(z_{ve})\|^2 \le 1$ for all $t > 0$. For an LTI system, the norm of $\mathbf{S}$ can be computed by its frequency response function. Therefore, the LTI system is passive if and only if

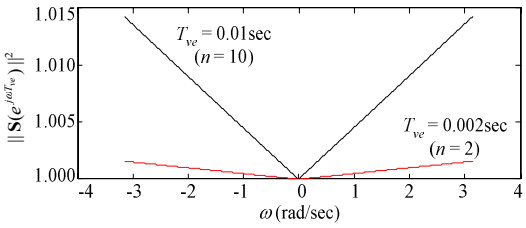

Fig. 2. Norm of scattering matrix (T = 0.001sec).

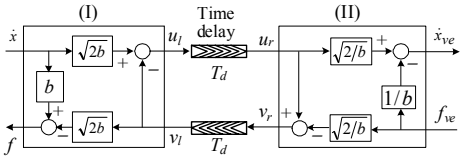

Fig. 3 Scattered communication line

$$\begin{aligned}\|\mathbf{S}(z_{ve})\|^2 &= \sup_{\omega}\|\mathbf{S}(e^{j\omega T_{ve}})\|^2 \\ &= \sup_{\omega}\lambda_{\max}(\mathbf{S}^*(e^{j\omega T_{ve}})\mathbf{S}(e^{j\omega T_{ve}})) \le 1\end{aligned}, \tag{7}$$

where $\lambda_{max}(\cdot)$ represents the largest eigenvalue and $\mathbf{S}^*$ denotes the complex conjugate transpose of $\mathbf{S}$.

Due to its huge size, verifying the passivity of $\mathbf{H}(z_{ve})$ using analytical approaches may not be very easy (for example, if n = 10, $\mathbf{H}(z_{ve})$ has 20×20 elements). Numerical computation of (7) for the scattering matrix of (5) was performed, and the results are shown in Fig. 2. It was found that $\|\mathbf{S}(e^{j\omega T_{ve}})\|^2 \ge 1$ for all ω. Hence, the rate transitions on the power variables such as velocity and force generate energy. As T_{ve} increases, $\|\mathbf{S}(e^{j\omega T_{ve}})\|^2$ also assumes larger values. Therefore, any controller (i.e., $G_c(z)$ shown in Fig. 1) is required to stabilize the system.

It is noted that damping is usually applied to $G_c(z)$ to stabilize a haptic system. As T_{ve} increases, more energy is generated, thus requiring a larger damping. A human operator is then likely to feel the damping effects in the free space in which no reaction force is generated (i.e., f_{ve} = 0) by VE.

III. Wave Variables

The wave variables have been introduced by Niemeyer and Slotine on the basis of the scattering parameters of the network theory and passivity formalism [8, 9]. Figure 3 illustrates part of a haptic interface in which the communication time delay exists at the wave variables. The wave variable with the subscript l (or r) denotes the wave variable of the haptic controller (or VE). The wave variables for a haptic controller are related to the power variables by

$$u_l = (b\dot{x} + f)/\sqrt{2b},\ \ v_l = (b\dot{x} - f)/\sqrt{2b}\ , \tag{8}$$

where b is the wave impedance that is an arbitrary positive constant that determines the behavior of the communication line. More details on the wave impedance can be referred to [9]. The wave variables for VE can be related to the power variables by

$$\dot{x}_{ve} = (u_r + v_r)/\sqrt{2b},\ \ f_{ve} = b(u_r - v_r)/\sqrt{2b} \tag{9}$$

Hence, the wave transforms (I) and (II) in Fig. 3 have an inverse relationship with each other. The power input of each wave transform can be derived as follows:

$$\dot{x}(t)f(t) = \{u_l(t)^2 - v_l(t)^2\}/2 \tag{10a}$$

$$\{u_r(t)^2 - v_r(t)^2\}/2 = \dot{x}_{ve}(t)f_{ve}(t) \tag{10b}$$

If no time delay exists in the communication channel, then $u_l = u_r$ and $v_l = v_r$ and thus (10a) is equal to (10b), in which case the wave transform delivers energy without any loss. Suppose that time delay exists as shown in Fig. 3. Then, $u_r(t) = u_l(t - T_d)$ and $v_l(t) = v_r(t - T_d)$. With these definitions and Eq. (10), the stored energy of the interface shown in Fig. 3 is computed by

$$E(t) = \frac{1}{2}\int_{t-T_d}^{t}\{u(\tau)^2 + v(\tau)^2\}d\tau \ge 0\,, \tag{11}$$

where T_d denotes the time delay. Note that a system is stable when $E(t) \ge 0$ for all t. Since (11) is always greater than zero, the energy is stored by the time delays on the wave variables. Hence, the time delays on the wave variables become passive elements, whereas those on the power variables are active. It has been reported that damping effects occur due to the distorted wave signal (i.e., delayed signal) during the time delay [9].

For a discrete-time system, the effect of $f(kT)$ on the energy is measured at the instant $(k+1)T$, since $f(kT)$ is computed at kT and applied during $kT \le t < (k+1)T$. To avoid this mismatch in the time instants, the following notation is used:

$$\dot{x}(kT) = \{x((k+1)T) - x(kT)\}/T \tag{12}$$

Then (10a) in a discrete form is obtained by

$$\dot{x}(kT)f(kT) = \{u_l(kT)^2 - v_l(kT)^2\}/2\,. \tag{13}$$

Similarly, Eq. (10b) can be computed in a discrete form. For more details on the discrete-time scattering, refer to [10].

IV. Multirate Wave Transform

In Section 2, the effects of rate transitions (i.e., downsampling and upsampling) on the power variables were investigated, and it was demonstrated that the rate transitions generate energy. Through the multirate modeling, downsampling was derived as a series of time delays. Since the time delay in the wave variables a passive element, it can be expected that the rate transitions on the wave variables will also be passive. In this section, the passivity of the rate transition on the wave variables is verified.

As shown in Fig. 4, the downsampler and upsampler are located at the wave variables. The downsampling with the sampling period T_{ve} is performed on the wave variable u, while the upsampling with the sampling period T on the wave variable v. In this case, let $n = T_{ve}/T$.

To verify the passivity, an input-output vector form will be derived. From (8) and (9), lifted forms are obtained, as follows:

$$\sqrt{2b}\tilde{\dot{x}}(k_{ve},0)=\tilde{u}_l(k_{ve},0)+\tilde{v}_l(k_{ve},0) \quad (14a)$$

$$b\tilde{x}(k_{ve},0)-\tilde{f}(k_{ve},0)=\sqrt{2b}\tilde{v}_l(k_{ve},0) \quad (14b)$$

$$2\tilde{f}_{ve}(k_{ve},0)/\sqrt{2b}=\tilde{u}_r(k_{ve},0)-\tilde{v}_r(k_{ve},0) \quad (14c)$$

$$2\tilde{u}_r(k_{ve},0)/\sqrt{2b}=\tilde{x}_{ve}(k_{ve},0)+\tilde{f}_{ve}(k_{ve},0)/b \quad (14d)$$

where $\tilde{x}(k_{ve},0)=[\dot{x}(k_{ve},0) \ \cdots \ \dot{x}(k_{ve},n-1)]^T \in R^n$,
$\tilde{f}(k_{ve},0)=[f(k_{ve},0) \ \cdots \ f(k_{ve},n-1)]^T \in R^n$,
$\tilde{u}_l(k_{ve},0)=[u_l(k_{ve},0) \ \cdots \ u_l(k_{ve},n-1)]^T \in R^n$,
$\tilde{v}_l(k_{ve},0)=[v_l(k_{ve},0) \ \cdots \ v_l(k_{ve},n-1)]^T \in R^n$,
$\tilde{\dot{x}}_{ve}(k_{ve},0)=[\dot{x}_{ve}(k_{ve},0) \ \cdots \ \dot{x}_{ve}(k_{ve},0)]^T \in R^n$,
$\tilde{f}_{ve}(k_{ve},0)=[f_{ve}(k_{ve},0) \ \cdots \ f_{ve}(k_{ve},0)]^T \in R^n$,
$\tilde{u}_r(k_{ve},0)=[u_r(k_{ve},0) \ \cdots \ u_r(k_{ve},0)]^T \in R^n$, and
$\tilde{v}_r(k_{ve},0)=[v_r(k_{ve},0) \ \cdots \ v_r(k_{ve},0)]^T \in R^n$.

Since $v_l(k_{ve}, i)$ is obtained from the interpolation (or upsampling) of $v_r(k_{ve},0)$, which has a constant value during the sampling period T_{ve}, $\tilde{v}_l(k_{ve},0)=\tilde{v}_r(k_{ve},0)$. Adding (14a) to (14c), the following relation is obtained:

$$\sqrt{2b}\tilde{\dot{x}}(k_{ve},0)+\frac{2}{\sqrt{2b}}\tilde{f}_{ve}(k_{ve},0)=\tilde{u}_l(k_{ve},0)+\tilde{u}_r(k_{ve},0) \quad (15)$$

The lifted wave variable $\tilde{u}_r(k_{ve},0)$ can be rewritten with $\tilde{u}_l(k_{ve},0)$ and a series of time delays, such as (4), as follows:

$$\tilde{u}_r(k_{ve},0)=\mathbf{P}\tilde{u}_l(k_{ve},0), \quad (16)$$

where $\mathbf{P}$ was given in (4). Substitution of (16) into (15) yields

$$\sqrt{2b}\tilde{\dot{x}}(k_{ve},0)+2\tilde{f}_{ve}(k_{ve},0)/\sqrt{2b}=(\mathbf{I}_n+\mathbf{P})\tilde{u}_l(k_{ve},0) \quad (17a)$$

$$\tilde{u}_l(k_{ve},0)=(\mathbf{I}_n+\mathbf{P})^{-1}\{\sqrt{2b}\tilde{\dot{x}}(k_{ve},0)+\frac{2}{\sqrt{2b}}\tilde{f}_{ve}(k_{ve},0)\} \quad (17b)$$

With (16) and (17b), (14d) is rewritten by

$$\begin{aligned}&\mathbf{P}(\mathbf{I}_n+\mathbf{P})^{-1}\{\sqrt{2b}\tilde{\dot{x}}(k_{ve},0)+2\tilde{f}_{ve}(k_{ve},0)/\sqrt{2b}\}\\&=\sqrt{2b}\tilde{x}_{ve}(k_{ve},0)/2+\tilde{f}_{ve}(k_{ve},0)/\sqrt{2b}\end{aligned} \quad (18)$$

Eliminating $\tilde{v}_l(k_{ve},0)$ from (14a) and (14b) yields

$$b\tilde{x}(k_{ve},0)+\tilde{f}(k_{ve},0)=\sqrt{2b}\tilde{u}_l(k_{ve},0) \quad (19)$$

Substitution of (17b) into (19) yields

$$\begin{aligned}&b\tilde{x}(k_{ve},0)+\tilde{f}(k_{ve},0)\\&=2(\mathbf{I}_n+\mathbf{P})^{-1}\{b\tilde{x}(k_{ve},0)+\tilde{f}_{ve}(k_{ve},0)\}\end{aligned} \quad (20)$$

Equations (18) and (20) can be rewritten as

$$\begin{aligned}&\tilde{f}(k_{ve},0)=\\&b\{2(\mathbf{I}_n+\mathbf{P})^{-1}-\mathbf{I}_n\}\tilde{x}(k_{ve},0)+2(\mathbf{I}_n+\mathbf{P})^{-1}\tilde{f}_{ve}(k_{ve},0)\end{aligned} \quad (21)$$

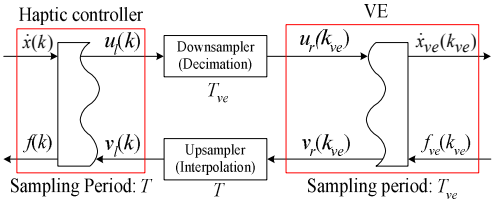

Fig. 4. Multirate wave transform.

$$\begin{aligned}&\tilde{\dot{x}}_{ve}(k_{ve},0)\\&=2\mathbf{P}(\mathbf{I}_n+\mathbf{P})^{-1}\tilde{\dot{x}}(k_{ve},0)\\&\quad+\{2\mathbf{P}(\mathbf{I}_n+\mathbf{P})^{-1}-\mathbf{I}_n\}\tilde{f}_{ve}(k_{ve},0)/b\end{aligned} \quad (22)$$

With (21) and (22), an input-output vector form is obtained by

$$\mathbf{H}(z_{ve})\mathbf{x}=\mathbf{y}, \quad (23)$$

where $\mathbf{H}(z_{ve})=\begin{bmatrix}b\{2(\mathbf{I}_n+\mathbf{P})^{-1}-\mathbf{I}_n\} & 2(\mathbf{I}_n+\mathbf{P})^{-1}\\ -2\mathbf{P}(\mathbf{I}_n+\mathbf{P})^{-1} & -\{2\mathbf{P}(\mathbf{I}_n+\mathbf{P})^{-1}-\mathbf{I}_n\}/b\end{bmatrix}\in R^{2n\times 2n}$, the input vector $\mathbf{x}=\{\tilde{\dot{x}}(k_{ve},0), \ \tilde{f}_{ve}(k_{ve},0)\}^T\in R^{2n}$, and the output vector $\mathbf{y}=\{\tilde{f}(k_{ve},0), \ -\tilde{\dot{x}}_{ve}(k_{ve},0)\}^T\in R^{2n}$.

To verify the passivity of $\mathbf{H}(z_{ve})$, a scattering matrix of $\mathbf{H}(z_{ve})$ is computed. Since $\mathbf{H}(z_{ve})$ increases in size as n increases, $\mathbf{H}(z_{ve})$ is reconfigured for easy computation of the scattering matrix. From the definition of $\mathbf{H}(z_{ve})$, $\mathbf{H}(z_{ve})$ is computed by

$$\mathbf{H}(z_{ve})=\left[\begin{array}{ccc|ccc}0 & \mathbf{0}^T & 0 & 1 & \mathbf{0}^T & 0\\ \mathbf{0} & \ddots & \mathbf{0} & \mathbf{0} & \ddots & \mathbf{0}\\ 0 & \mathbf{0}^T & b\frac{z_{ve}^{(n-1)/n}-1}{z_{ve}^{(n-1)/n}+1} & 0 & \mathbf{0}^T & \frac{2z_{ve}^{(n-1)/n}}{z_{ve}^{(n-1)/n}+1}\\ \hline -1 & \mathbf{0}^T & 0 & 0 & \mathbf{0}^T & 0\\ \mathbf{0} & \ddots & \mathbf{0} & \mathbf{0} & \ddots & \mathbf{0}\\ 0 & \mathbf{0}^T & -\frac{2}{z_{ve}^{(n-1)/n}+1} & 0 & \mathbf{0}^T & -\frac{z_{ve}^{(n-1)/n}-1}{b(z_{ve}^{(n-1)/n}+1)}\end{array}\right]. \quad (24)$$

$\mathbf{H}(z_{ve})$ can be divided into four diagonal matrix as shown in (24). Let the input vector $\mathbf{x}_m=\{\dot{x}(k_{ve},0), \ f_{ve}(k_{ve},0) \ \cdots \ \dot{x}(k_{ve},n-1), \ f_{ve}(k_{ve},n-1)\}^T\in R^{2n}$ and the output vector $\mathbf{y}_m=\{f(k_{ve},0), \ -\dot{x}_{ve}(k_{ve},0) \ \cdots \ f(k_{ve},n-1), \ -\dot{x}_{ve}(k_{ve},n-1)\}^T \in R^{2n}$. The new input and output vectors satisfy the condition that $\mathbf{x}^T\mathbf{y}=\mathbf{x}_m{}^T\mathbf{y}_m$. With the new input and output vectors and (24), the new operator $\mathbf{H}_m(z_{ve})$ is obtained as follows:

$$\mathbf{H}_m(z_{ve})=\begin{bmatrix}H_{m11}(z_{ve}) & 0 & \cdots & 0\\ 0 & H_{m22}(z_{ve}) & & \vdots\\ \vdots & & \ddots & 0\\ 0 & \cdots & 0 & H_{mnn}(z_{ve})\end{bmatrix}\in R^{2n\times 2n}, \quad (25)$$

where

$$H_{mii}(z_{ve})=\begin{bmatrix}b\{z_{ve}^{(i-1)/n}-1\}/\{z_{ve}^{(i-1)/n}+1\} & \{2z_{ve}^{(i-1)/n}\}/\{z_{ve}^{(i-1)/n}+1\}\\ -2/\{z_{ve}^{(i-1)/n}+1\} & -\{z_{ve}^{(i-1)/n}-1\}/\{b(z_{ve}^{(i-1)/n}+1)\}\end{bmatrix}$$

for $i=1,\cdots,n$. From (6), the scattering matrix is obtained by

$$\mathbf{S}(z_{ve}) = (\mathbf{H}_m(z_{ve}) - \mathbf{I}_{2n})(\mathbf{I}_{2n} + \mathbf{H}_m(z_{ve}))^{-1} = \begin{bmatrix} S_{11}(z_{ve}) & 0 & \cdots & 0 \\ 0 & \ddots & & \vdots \\ \vdots & & \ddots & 0 \\ 0 & \cdots & 0 & S_{nn}(z_{ve}) \end{bmatrix} \in R^{2n\times 2n}, \quad (26)$$

where $S_{ii}(z_{ve}) = (H_{mii} - \mathbf{I}_2)(H_{mii} + \mathbf{I}_2)^{-1}$

$$= \begin{bmatrix} \dfrac{(b^2-1)(z_{ve}^{(i-1)/n}-1)}{(b+1)^2 z_{ve}^{(i-1)/n} - (b-1)^2} & \dfrac{4bz_{ve}^{(i-1)/n}}{(b+1)^2 z_{ve}^{(i-1)/n} - (b-1)^2} \\ \dfrac{-4b}{(b+1)^2 z_{ve}^{(i-1)/n} - (b-1)^2} & \dfrac{-(b^2-1)(z_{ve}^{(i-1)/n}-1)}{(b+1)^2 z_{ve}^{(i-1)/n} - (b-1)^2} \end{bmatrix} \text{ for } i = 1,\cdots,n.$$

To compute the norm of $\mathbf{S}(z_{ve})$, $\mathbf{S}^*(e^{j\omega T_{ve}})\mathbf{S}(e^{j\omega T_{ve}})$ should be obtained. Let $q \equiv e^{j\omega T} = \cos(\omega T) + j\sin(\omega T)$. Then, $e^{j\omega T_{ve}} = e^{j\omega nT} = q^n$ ($n = T_{ve}/T$) and $\mathbf{S}^*(e^{j\omega T_{ve}})\mathbf{S}(e^{j\omega T_{ve}})$ is obtained by

$$\mathbf{S}^*(q^n)\mathbf{S}(q^n) = \begin{bmatrix} A_{11}(q^n) & \cdots & 0 \\ \vdots & \ddots & \vdots \\ 0 & \cdots & A_{nn}(q^n) \end{bmatrix} \quad (27)$$

where $A_{ii}(q^n) = \mathbf{S}_{ii}^*(q^n)\mathbf{S}_{ii}(q^n)$ for $i = 1,\cdots,n$. Expanding $A_{ii}(q^n)$ (see Appendix section) yields

$$A_{ii}(q^n) = \begin{bmatrix} 1 & 0 \\ 0 & 1 \end{bmatrix} \text{ for } i = 1,\cdots,n. \quad (28)$$

Thus, equation (27) becomes the identity matrix, in which the eigen values are all equivalent to 1. Hence, the scattering matrix of (26) satisfies the condition that $\sup_{\omega} \lambda_{\max}(\mathbf{S}^*(e^{j\omega T_{ve}})\mathbf{S}(e^{j\omega T_{ve}})) \le 1$. It can be concluded from these results that the rate transitions on the wave variables shown in Fig. 4 are passive regardless of b, n, ω, and T.

Note for real implementation that sample and hold at the haptic controller and downsampling and upsampling between the haptic controller and VE are conducted as shown in Fig. 1. Since the sampling period of VE is usually greater than that of the haptic controller, it can be estimated that the more energy is generated at the rate transition (downsampling and upsampling) rather than that of sample and hold at the haptic controller. From the result that the rate transitions on the wave variables are passive, we can eliminate the effect of the rate transition which dominantly generates energy. However, the sample and hold at the haptic controller also generate energy. To build stable haptic interface, it is required that the generated energy from active elements is less than the absorbed or stored energy by passive elements as generally known. In most cases, the human operator considered to be passive [20] and VE is design with passive elements such as spring. Hence, to guarantee the stability, energy absorbed by the rate transition on the wave variables should be greater than generated energy from the sample and hold at the haptic controller. This condition would say that there is stability range associated with b, n, and T.

V. Experiments and Discussions

A. Experimental setup

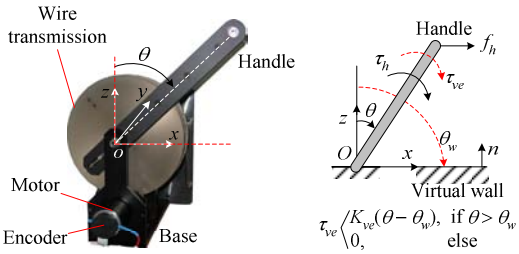

(a) Experimental device (b) Virtual environment

Fig. 5. Experimental setup.

A 1-DOF haptic device was developed for conducting the experiments, as shown in Fig. 5(a). An aluminum-alloy handle was attached at the output axis of the wire transmission to minimize the moving mass, rotating about the origin O. In the figure, θ and $\dot{\theta}$ represented the rotating angle of the handle and its rotational velocity, respectively. An optical encoder mounted at the motor axis sensed the rotational motion of the handle.

A virtual wall was implemented with the surface located at $\theta_w = 90^o$, as shown in Fig. 5(b). A vector, n, denoted the surface normal vector of the virtual wall. A spring-damper model was applied to the virtual wall, in which the spring constant, K_{ve}, was set to 10^2Nm/rad and damping coefficient, D_{ve}, was set to 0.5Nm·sec/rad. The virtual torque, τ_{ve}, was computed by $K_{ve}(\theta - \theta_w) + D_{ve}\dot{\theta}$, if $\theta > \theta_w$ (i.e., penetration occurs). Otherwise, τ_{ve} would be set to zero. A hand-force (or torque) input f_h (or τ_h) was provided to move the handle in the counter-clockwise direction. In the experiments, the sampling period of VE was set at 0.05 sec. Note that time delay in a communication line was not implemented during experiments to clearly show the effects of the multirate wave transform.

B. Displaying virtual wall

Fig. 6 shows the experimental results of the proposed haptic interface. Since the multirate wave transform was confirmed to be passive in Section 4, a stable force display was achieved. In this case, the wave impedance b and the ratio n were experimentally determined to get values of 1.5Nm·sec/rad and 50, respectively. The energy of device remained at the positive (passive) region. Note that The energy of VE was computed by the summation of $\dot{x}_{ve}(k_{ve}T_{ve})f_{ve}(k_{ve}T_{ve})T_{ve}$ while that of the device was obtained by the summation of $\dot{x}(kT)f(kT)T$. After the initial contact, the wave variable u obtained the same magnitude as that of v with the opposite sign. It has been reported that the wave variables have the same magnitude, but they have opposite signs at the steady state [9].

VI. Conclusions

This paper proposes a control method that attempts to overcome the instability arising from the low update rates of VE and time delay in a communication line. Since sample and hold (decimation and interpolation) in the discrete time domain can be represented by a series of time delays, the passive nature of time delay on the wave variables is applied. By computing the norm of scattering matrix, it was verified that rate transitions (digital sample and hold) on the wave

variables are passive. With this result, a stable haptic interface was derived with the multirate wave transform. It is shown from experiment that stable force display can be achieved with the multirate wave transform.

In the case no time delay exists in a communication line, the amount of the restored energy at the multirate wave transform can be determined by the wave impedance, b, the ratio of sampling intervals, n, sampling period, T. To guarantee the stability of a haptic interface, the restored energy at the multirate wave transform must be greater than the generated energy by the sample & hold for continuous time domain. Therefore, it is necessary to find ranges of b and n satisfying the passivity condition.

REFERENCES

[1] R. B. Gillespie and M. R. Cutkosky., "Stable User-Specific Rendering of the Virtual Wall," Proc. ASME Int. Mech. Eng. Conf. and Exp., Atlanta, GA, Nov. 1996, DSC-Vol. 58, pp. 397-406.

[2] J. E. Colgate and G. G. Schenkel, "Passivity of a class of sampled-data systems: Application to haptic interfaces," J. of Robotic Systems, vol. 14, no. 1, pp. 37-47, Jan. 1997.

[3] R. J. Adams and B. Hannaford, "Stable haptic interaction with virtual environments," IEEE Trans. Robot. Automat., vol. 5, no. 3, pp. 465-474, June 1999.

[4] B. E. Miller, J. E. Colgate, and R. A. Freeman, "Environment delay in haptic systems," Proc. IEEE Int. Conf. Robot. Automat., San Francisco, CA, April 2000, pp. 2434-2439.

[5] B. Hannaford and J. Ryu, "Time-domain passivity control of haptic interfaces," IEEE Trans. Robot. Automat., vol. 18, no. 1, pp. 1-10, Feb. 2002.

[6] S. Stramigioli, C. Secchi, A. J. van der Schaft, and C. Fantuzzi, " A novel theory for sample data system passivity," Proc. IEEE/RSJ Int. Conf. Intelligent Robotics and systems, Lausanne, Switzerland, Sept. 2002, vol. 2, pp. 1936–1941.

[7] R. Anderson, and M. Spong, "Bilateral control of teleoperation with time delay," IEEE Trans. Automatic control, vol. 34, no. 5, pp. 494-501, May 1989.

[8] G. Niemeyer, and J. E. Slotine, "Stable Adaptive Teleoperation," IEEE J. of Oceanic Eng., vol. 16, no.1, pp.152-162, January, 1991.

[9] G. Niemeyer, Using Wave Variables in Time Delayed Force Reflecting Teleoperation, Phd. Dissertation, Dept. Aeronautics and Astronautics, MIT, Cambridge, MA, 1996.

[10] C. Secchi, S. Stramigioli, and C. Fantuzzi, "Digital Passive Geometric Telemanipulation," Proc. IEEE Int. Conf. Robot. Automat Taipei, Taiwan, Sept. 2003, pp. 3290–3295.

[11] Y. Yokokohji, T. Imaida, and T. Yoshikawa, "Bilateral control with energy balance monitoring under time-varying communication delay," Proc. IEEE Int. Conf. Robot. Automat., San Francisco, CA, April 2000, pp. 2684-6289.

[12] S. Munir and W. J. Book, "Internet-based teleoperation using wave variables with prediction," IEEE/ASME Trans. Mechatronics, vol. 7, no. 2, pp. 124 – 133, June 2002.

[13] J. E. Colgate and J. M. Brown, "Factors Affecting the Z-Width of a Haptic Display," Proc. IEEE Int. Conf. Robot. Automat., San Diego, CA, May 1994, pp. 3205-3210.

[14] F. Barbagli, D. Prattichizzo, and K. Salisbury, "Multirate analysis of haptic interaction stability with deformable objects," Proc. IEEE Conf. Decision and Control, Las Vegas, Nevada, Dec. 2002, pp. 917-922.

[15] O. R. Astley and V. Hayward, "Multirate haptic simulation achieved by coupling finite element meshes through norton equivalents," Proc. IEEE Int. Conf. Robot. Automat., Leuven, Belgium, May 1998, pp. 989-994.

[16] S. H. Lee, C. C. Chung, and S. M. Suh, "Multirate digital control for high track density magnetic disk drives," IEEE Trans. Magnetics, vol. 39, no. 2, pp. 832-837, March 2003.

[17] R. Ravi, P. P. Khargonekar, K. D. Minto, and C. N. Nett, "Controller parameterization for time-varying multirate plants," IEEE Trans. Automatic Control, vol. 35, no. 11, pp. 1259-1262, Nov. 1990.

[18] K. J. Åström and B. Wittenmark, *Computer-Controlled Systems—Theory and Design*. Englewood Cliffs, NJ: Prentice Hall, 1997.

[19] S. S. Haykin, *Active Netwok Theory*, NY: Addison-Wesley, 1970.

[20] N. Hogan, "Controlling impedance at the man/machine," Proc. IEEE Int. Conf. Robot. Automat., Scottsdale, AZ, May 1989, pp. 1626–1631.

APPENDIX

A. Computing $A_{ii}(q^n)=\mathbf{S}_{ii}^*(q^n)\mathbf{S}_{ii}(q^n)$

$$\mathbf{S}_{ii}(q^n)=\frac{1}{C}\begin{bmatrix}(b^2-1)(q^{i-1}-1) & 4bq^{i-1}\\ -4b & -(b^2-1)(q^{i-1}-1)\end{bmatrix} \tag{A1}$$

$$\mathbf{S}_{ii}^*(q^n)=\frac{1}{\overline{C}}\begin{bmatrix}(b^2-1)(\overline{q^{i-1}}-1) & -4b\\ 4b\overline{q^{i-1}} & -(b^2-1)(\overline{q^{i-1}}-1)\end{bmatrix} \tag{A2}$$

where $C=(b+1)^2q^{i-1}-(b-1)^2$, $\overline{C}=(b+1)^2\overline{q^{i-1}}-(b-1)^2$.

$$\overline{C}C=2(b^2-1)^2+16b^2-(b^2-1)^2(\overline{q^{i-1}}+q^{i-1}) \tag{A3}$$

$$\begin{aligned}A_{ii,11}(q^n)&=\{(b^2-1)^2(\overline{q^{i-1}}-1)(q^{i-1}-1)+16b^2\}/\overline{C}C\\&=\{2(b^2-1)^2+16b^2-(b^2-1)^2(\overline{q^{i-1}}+q^{i-1})\}/\overline{C}C\\&=1\end{aligned} \tag{A4}$$

$$\begin{aligned}&A_{ii,12}(q^n)\\&=\{4b(b^2-1)q^{i-1}(\overline{q^{i-1}}-1)+4b(b^2-1)(q^{i-1}-1)\}/\overline{C}C\\&=4b(b^2-1)\{q^{i-1}(\overline{q^{i-1}}-1)+(q^{i-1}-1)\}/\overline{C}C\\&=0\end{aligned} \tag{A5}$$

$$\begin{aligned}&A_{ii,21}(q^n)\\&=\{4b(b^2-1)\overline{q^{i-1}}(q^{i-1}-1)+4b(b^2-1)(\overline{q^{i-1}}-1)\}/\overline{C}C\\&=4b(b^2-1)\{q^{i-1}(q^{i-1}-1)+(\overline{q^{i-1}}-1)\}/\overline{C}C\\&=0\end{aligned} \tag{A6}$$

$$\begin{aligned}&A_{ii,22}(q^n)\\&=\{16b^2\overline{q^{i-1}}q^{i-1}+(b^2-1)^2(\overline{q^{i-1}}-1)(q^{i-1}-1)\}/\overline{C}C\\&=\{2(b^2-1)^2+16b^2-(b^2-1)^2(\overline{q^{i-1}}+q^{i-1})\}/\overline{C}C\\&=1\end{aligned} \tag{A7}$$

Hence, $A_{ii}(q^n)=\begin{bmatrix}A_{ii,11}(q^n) & A_{ii,12}(q^n)\\ A_{ii,21}(q^n) & A_{ii,22}(q^n)\end{bmatrix}=\begin{bmatrix}1 & 0\\ 0 & 1\end{bmatrix}$ for all i.

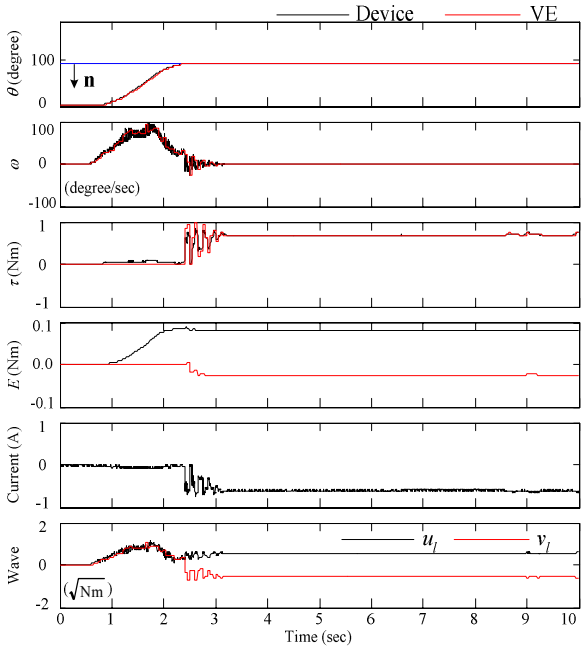

Fig. 6. Experimental results of the proposed haptic interface with multirate wave transform (T = 0.001sec, T_{ve} = 0.05sec, K = 10^2Nm/rad, D_{ve} = 0.5Nmsec/rad, b = 1.5Nmsec/rad).